Fabrication of photothermally actuated microheater with SU-8/Cu composite

OPEN ACCESS
IOP Publishing
Journal of Micromechanics and Microengineering
J. Micromech. Microeng. **31** (2021) 095007 (11pp)
https://doi.org/10.1088/1361-6439/ac1996

Fabrication of photothermally actuated microheater with SU-8/Cu composite

Tasuku Nakahara*, Kazuki Ise and Kazuyuki Minami

Department of Mechanical Engineering, Yamaguchi University, Yamaguchi, Japan

E-mail: tasuku@yamaguchi-u.ac.jp

Received 12 February 2021, revised 5 July 2021
Accepted for publication 30 July 2021
Published 13 August 2021

Abstract

The photothermally actuated microheaters have been studied for various applications. In particular, microheaters using composites mixed with polymer and particles were developed for a microrobot and thermally responsive structures. However, the structures have been fabricated by soft lithography process, which needs multiple steps. Here, we propose a microheater fabricated using a photosensitive composite, which is a mixture of the photosensitive resin SU-8 and Cu microparticles. The composite structures fabricated by one step photolithography exhibited a rise of temperature due to the photothermal effect, which was induced by the observation system of an inverted fluorescent microscope. In evaluating the patterning accuracy of the composite, although the line-and-space pattern formed was a minimum of 30 μm, the fabricated patterns involved a dimensional error of 5%–25%. The composite with 50 wt% Cu particles of 1 μm showed a maximum temperature of 55.7 °C in our experiments. The micropatterns of the microheater were fabricated and showed a rise of temperature of 16 °C–46 °C. In addition, the time response of the rising temperature was approximately 1 s. Thus, the proposed microheater could be useful for applications in which a change of temperature in the range of 10 °C–40 °C.

Supplementary material for this article is available online

Keywords: photosensitive composite, SU-8, copper particle, lab-on-a-chip, photothermal effect

(Some figures may appear in colour only in the online journal)

1. Introduction

The photothermally actuated microheaters have been studied for applications such as an actuator [1, 2], thermoelectric conversion [3], and control of activity in proteins [4]. In particular, microheaters using composites mixed with polymer and particles have been developed for a microrobot and thermally responsive structures [5–10]. Although these previous studies reported microdevices having the photothermally actuated heater, the structures have been fabricated by soft lithography process, which needs multiple steps such as a making mold, pouring polymer solution into the mold, and removing mold after crosslinking the polymer. To achieve the simple fabrication process for making microdevices, the utilisation of photosensitive composites, which are a mixture of photosensitive resin SU-8 [11, 12] and functional particles, has been studied. The photosensitive composites has both of a processablity for microfabrication and a functionality of particles. Therefore, microdevices with conductivity, magnetic properties, and improved mechanical properties can be fabricated with one step photolithography [13–16]. While these functional properties enabled the fabrication of microdevices such as micromirrors, micropumps, and microelectric circuits [17–22], there is no report for the microheater in our knowledge.

* Author to whom any correspondence should be addressed.

Hence, we propose a microheater fabricated using a photosensitive composite. The composite is a mixture of the photosensitive resin SU-8 and Cu microparticles. Cu particles are low cost and exhibit a light absorption in the visible light owing to surface plasmon resonance. Resonance effects can increase the temperature of the Cu particles [23]. Therefore, the microstructures fabricated by conventional photolithography show a rise of temperature due to light irradiation. The increased temperature of the Cu particles could be maintained in the composite because the low thermal conductivity of SU-8 acts as thermal insulator. To evaluate the processability of the composite, we analysed the transmittance, exposed thickness, and patterning accuracy. We also evaluated the photothermal effect of the composites to analyse different properties affected by the weight ratio and the diameter of the Cu particles. The microheater patterns were fabricated with conventional photolithography, and their properties were evaluated on the observation system of an inverted fluorescent microscope to investigate possible applications.

2. Materials and methods

2.1. Concept of proposed microheater

Figure 1 shows a schematic of the proposed microheater. The microheater was constructed with a coverslip and a composite made of photoresist and Cu particles. The composite has the processability of the photoresist, which enables the formation of micropatterns using photolithography, and functionality of the particles. The Cu particles exhibit a rise of temperature induced by the photothermal effect, which indicates that the Cu particles absorb light energy and convert it into thermal energy. Therefore, a rise of temperature is induced around the composite in a light irradiated area, as shown in figure 1 (area B). In contrast, no rise of temperature is observed in the irradiated area without the composite (area A) or the nonirradiated area with composite (area C). These characteristics enable the control of the temperature in a desirable microarea by altering the light irradiated area or pattern shape of microstructures.

2.2. Preparation method of composites

The composite was prepared by mixing a negative-type photoresist SU-8 (SU-8 3010, MicroChem) and Cu particles of approximately 1 or 5 μm in diameter (CUE08PB, CUE12PB, Kojundo Chemical Laboratory). First, SU-8 and a surfactant (DISPERBYK-111, BYK) were mixed using a planetary mixer (AR-100, Thinky) for 5 min. The surfactant volume was 5% of the weight of the mixing particles. The weights of the Cu particles were set at 10, 20, 30, 50, and 70 wt% for the entire weight of the composite in accordance with the experimental conditions. The SU-8 and particles were mixed using the mixer for 5 min, and the composite was degassed by a vacuum desiccator for 10 min to remove the bubbles. Sonication was then applied using an ultrasonic cleaner (MCS-2, AS ONE) to disperse the particles of the composite. Finally, the planetary mixing process was performed again.

2.3. Evaluation method for transmittance and exposed thickness of composites

Because the composite is a mixture of SU-8 and Cu particles, the transmittance of the composite is lower than that of SU-8 without particles. Therefore, evaluations of transmittance and exposed thickness of composites are important to fabricate a designed micro pattern by photolithography.

Composites prepared with Cu (10, 20, 30, 50, 70 wt%) and Cu (30, 50, and 70 wt%) were used to measure the transmittance and the exposed thickness, respectively. The prepared composites were spin-coated on coverslips (22 $\times$ 22 $\times$ 0.17–0.25 mm: C022222, Matsunami Glass) with approximately 10–15 and 30–40 μm in thickness for the evaluation of transmittance and the exposed thickness, respectively. Then, a prebake process (65 °C for 5 min, 95 °C for 30 min) was performed. After the prebake process, the entire spin-coated composite was exposed to an ultraviolet (UV) light from the back side of the coverslip. For the specimens of exposed thickness, a photomask with a rectangular pattern (8 $\times$ 15 mm) was used as shown in figure 2(a). In the fabrication of specimens for transmittance, the doses of UV light were set to 0.4, 0.4, 0.6, 0.8 and 1.2 J cm^{-2} for the composites with Cu of 10, 20, 30, 50 and 70 wt%, respectively. UV irradiance was measured using an UV meter (UIT-201, Ushio) with detector unit (UVD-365PD, Ushio). For the specimens of exposed thickness, the exposure doses were set to 0.4, 0.8, 1.2, 1.6, 2.0 J cm^{-2} and 0.4, 0.8, 1.2, and 1.6 J cm^{-2} for the composites with Cu particles of diameters of 1 and 5 μm, respectively. Then, a postexposure bake process (65 °C for 1 min, 95 °C for 5 min) was performed. The unexposed parts were removed by a developer with sonication for 5 min, and the exposed parts were retained on the coverslip. Finally, a hard bake (200 °C for 30 min) was performed. For a comparison in the evaluation of transmittance, the specimen using SU-8 was prepared using the same fabrication process. The exposure dose was set at 0.4 J cm^{-2}.

The thickness of the retained structures on the coverslip was measured using a high-precision noncontact depth measuring microscope (HISOMET II, Union Optical) or a stylus profiler (Dektak XT, Bruker), as shown in figure 2(b). We measured the exposed thickness at three points on the fabricated structures and calculated the average thickness. The transmittance measurements of the composites were performed using a spectrophotometer (V-730, JASCO). The wavelength range of measurement was set from 300 nm to 1100 nm. The data was normalized by the results of blank coverslip. To relate the transmittance to the thickness of the composites, the absorption coefficients of the composites were calculated using $T = \mathrm{e}^{-\alpha x}$ of Lambert–Beer's law, where T is the transmittance of the composite, e is Napier's constant, α is the absorption coefficient, and x is the thickness of the retained structure.

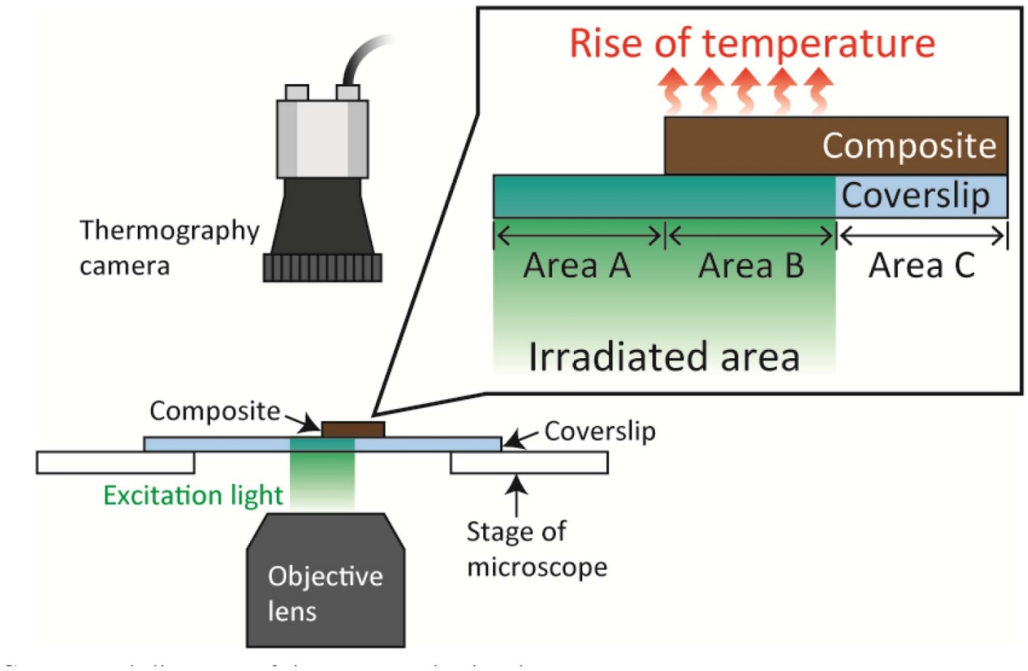

Figure 1. Conceptual diagram of the proposed microheater.

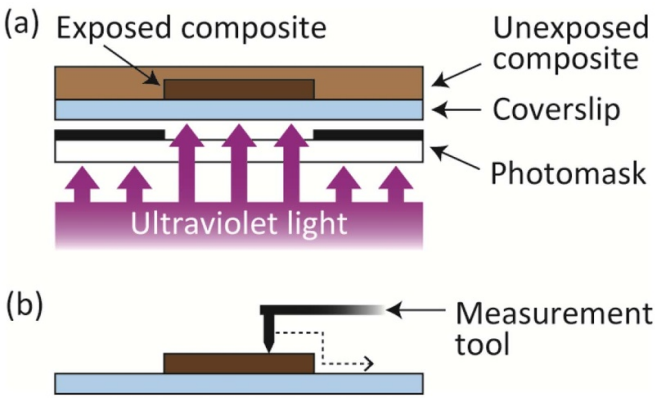

Figure 2. Experimental method for measuring the exposure thickness. (a) Schematic of the exposure from the back side. (b) Retained structure of the composite measured using a stylus profiler.

2.4. Evaluation method for patterning accuracy of composites

To measure the patterning accuracy of the composites, the specimens were fabricated by photolithography using a photomask with a line-and-space pattern, in which the space parts transmit UV light (line-and-space width: 10, 12, 15, 20, 25, 30, 40, and 50 μm). They were exposed to an UV light from the back side of the coverslip through a photomask. The doses of UV exposure were set to 0.6, 0.8, and 1.2 J cm^{-2} for the composites with Cu of 30, 50, and 70 wt%, respectively. Then, the postexposure bake and development processes were performed using the same procedure as mentioned above. The width of the fabricated line-and-space patterns was observed and measured using a high-precision noncontact depth-measuring microscope. In this experiment, we measured five lines and five spaces, and then calculated the average width for each specimen.

2.5. Evaluation method for photothermal effect of composites

To evaluate the photothermal effect of composites, specimens with a rectangular composite structure including Cu of 10, 20, 30, 50, and 70 wt% were prepared using the same process as described in section 2.3. The thickness of the structures was measured by the stylus profilers. The prepared specimen was set on a stage of an inverted fluorescent microscope (IX70, Olympus) incorporated with a light source (U-HGLGPS, Olympus). A 520–550 nm green light was irradiated to the specimen from a 100× objective lens (UPLSAPO100XO, Olympus) through a fluorescence filter cube (U-MWIG, Olympus). The irradiated area, approximately 265 μm in diameter, was set at the centre of the rectangular composite structure (8 × 15 mm) and at the boundary between the structure and glass area. A rise of temperature was observed and measured using a thermography camera (OPTPI640MO44T900, Optris) for the change of irradiances at 3.5, 7.0, 13, 28, 61, and 111 W cm^{-2}. The minimum spatial resolution of thermography camera is 28.8 μm. The temperatures were measured at each interval of ∼15 s after starting irradiation to evaluate them in a steady state. Irradiances through the objective lens were measured using an excitation irradiance adaptor (IX3-EXMAD, Olympus) equipped with an optical power meter (3664, Hioki) and a power sensor (9742-10, Hioki). For comparison, a specimen with a rectangular structure using SU-8 was prepared, and the temperature was measured in the centre of structure with irradiance at 111 W cm^{-2}.

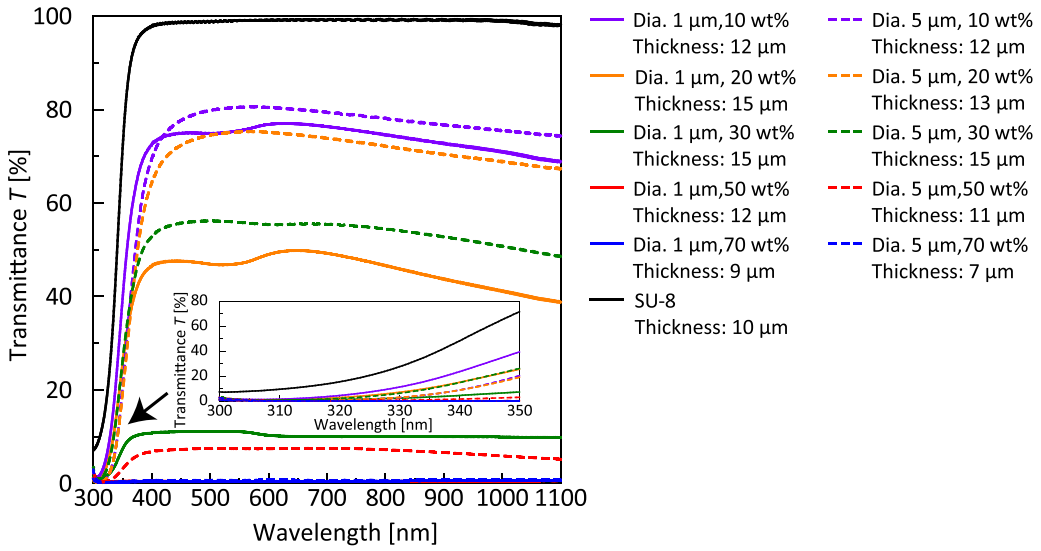

Figure 3. Measurement results of transmittance of composites and SU-8. The inserted graph is the enlarged results of transmittance in the range between 300 and 350 nm of wavelength.

2.6. Evaluation method of characteristics of microheater

To evaluate the characteristics of the composite structure as a microheater, circular composite structure with diameters of 100, 200, 400, 1000, and 2000 μm were fabricated by the same method as described in section 2.3. Briefly, the composite with 70 wt% of 1 μm diameter Cu particles was prepared and spin-coated on a coverslip. After the prebake process, the composite was exposed to UV light from the back side through the photomask with circular patterns. The circular structures were fabricated by performing the postexposure bake and development processes. Finally, a hard bake process was performed. The thicknesses of the fabricated structures were measured using a high-precision noncontact depth measuring microscope. The excitation light of 111 W cm^{-2} was irradiated at the centre of the circular structure, and the temperature was measured using a thermography camera, as described in section 2.5. To evaluate the time response of the change in temperature on the composite, the irradiance was switched between 0 and 111 W cm^{-2} with period of approximately 2 s in the 2000 μm circular structure.

3. Results and discussion

3.1. Evaluation results for transmittance and exposed thickness of composites

Figure 3 shows the measurement results of the transmittance for the composites and SU-8 at wavelengths from 300 to 1100 nm. The transmittance of the composites was lower than that of SU-8, and decreased with an increase of the weight ratio of Cu particles. The transmittance of the composite prepared with 1 μm diameter Cu particles significantly decreased with an increase of the weight ratio compared to that of the composite prepared with 5 μm diameter Cu particles. The composite with Cu particles of 1 μm in diameter may be existed more densely compared with that of 5 μm. It could be lead the results of lower transmittance in the composite using 1 μm particles at the visible light region. In the over 50 wt% of composite, especially using Cu particles with 1 μm of diameter, there could be almost no transmitted visible light. Figure 4 shows the absorption coefficients of the composites and SU-8 calculated by the Lambert–Beer law using the measured transmittance and thickness. There is a difference of trend between the results of transmittance and absorption coefficients because the absorption coefficients were affected by the thickness of composites. The thickness of SU-8 without particles was thinner than that of composites because the composite viscosity, which affects to the spin-coated thickness, were higher than SU-8 viscosity. The mixing particles or degas process could affect the increase of composites viscosity. In the wavelengths from 400 to 1100 nm, the absorption coefficients of the composites were larger than those of SU-8. The absorption coefficients of the composites with 1 μm diameter Cu particles were larger than those of the composite using 5 μm diameter Cu particles except 70 wt%. In the 70 wt% of composites, since there was almost no transmitted visible light, the difference of trend could be resulted from the difference of the composite thicknesses. The light absorption of Cu particles at wavelengths near 600 nm was reported by Chen *et al* [23]; the excitation wavelength of 520–550 nm could be absorbed by Cu particles in the composite. In the wavelength shorter than 365 nm, although SU-8 absorbs light for the crosslinking of the structure, the absorption coefficients of the composites were larger than that of SU-8 in this wavelength range. These results suggest that the exposed depth of composites to the UV light for patterning is smaller than that of SU-8, and a larger dose is required for patterning in the photolithography.

Figure 5(a) shows the fabricated specimen for evaluation of composite thickness by using Cu 70 wt% composite with 1 μm diameter. The composite pattern was formed and the edge of pattern was observed as shown in figure 5(b). Figure 6 shows the exposed thickness (mean $\pm$ standard deviation) of the composites, i.e. the structure thickness, for the exposure dose.

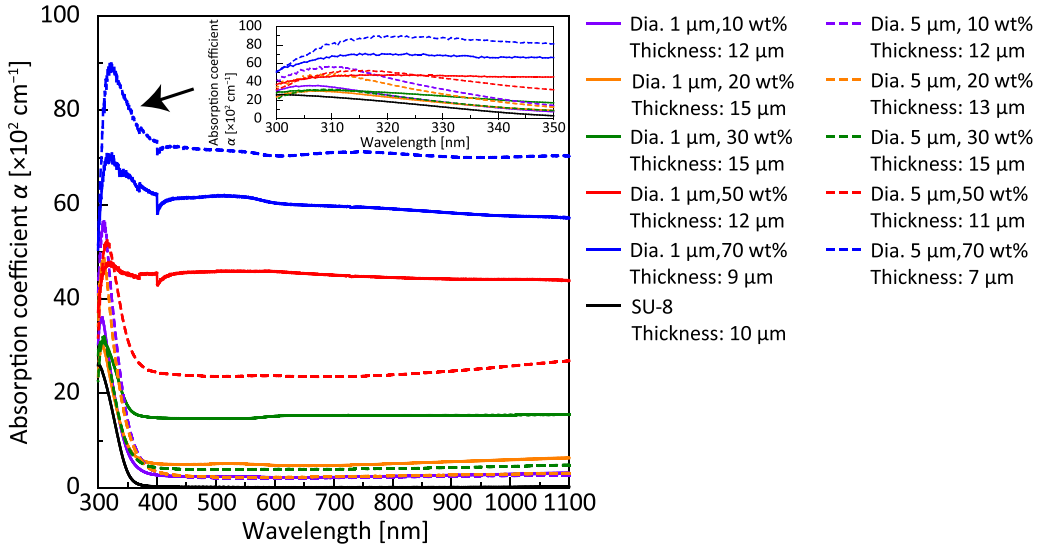

Figure 4. Absorption coefficient of composites and SU-8 calculated by Lambert–Beer law. The inserted graph is enlarged results of absorption coefficient in the range between 300 and 350 nm of wavelength.

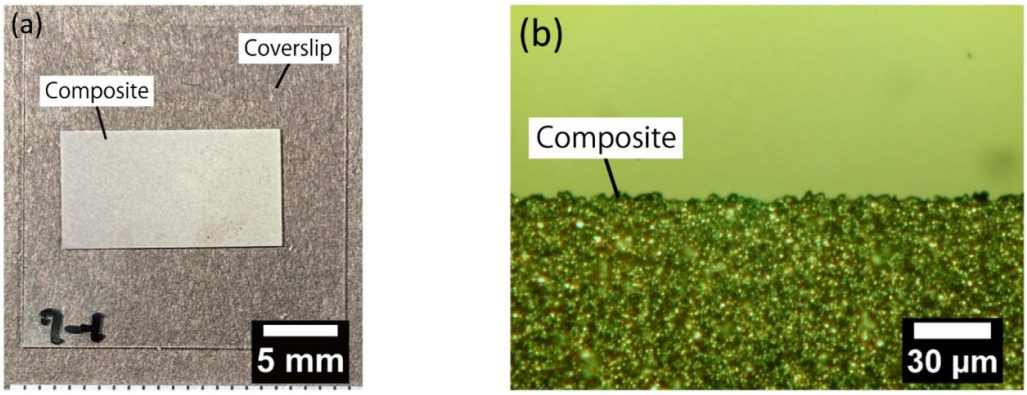

Figure 5. The fabricated specimen for evaluation of exposed thickness. The observation images are (a) entire view and (b) enlarged view at boundary between the composite and glass region.

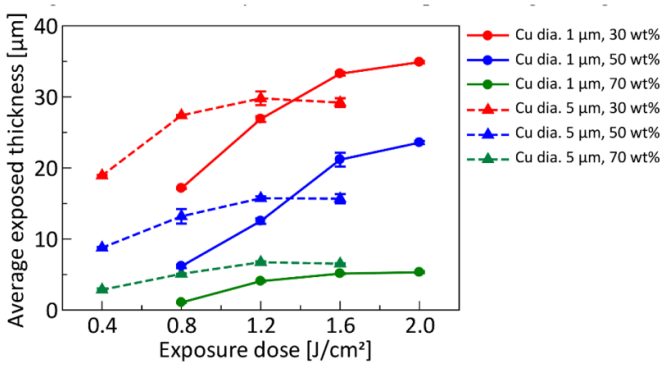

Figure 6. Composite thickness for different exposure doses.

Because the retained structures using the composites with 1 μm diameter Cu on the coverslip was not observed at an exposure dose of 0.4 J cm^{-2}, the thicknesses were not measured. It may be attributed to an insufficient exposure dose for fabricating the structures. For composites with 1 μm diameter Cu particles, the maximum values of exposed thicknesses with Cu of 30, 50, and 70 wt% were 34.9, 23.5, and 5.3 μm, respectively, at an exposure dose of 2.0 J cm^{-2}. On the other hand, for composites with 5 μm diameter Cu particles, the maximum values of exposed thicknesses were 29.8, 15.7, and 6.7 μm, respectively, at an exposure dose of 1.2 J cm^{-2}. The exposed thickness decreased with an increase of the weight ratio of Cu particles because of the absorption and reflection in the surface of Cu particles, which impeded the UV light from entering the surface to the interior of the composite. In addition, since there is almost same in exposed thicknesses with increase of exposure dose after reaching the maximum values of exposed thickness in each specimen, there is a limitation of the exposed depth in the composites according to the weight ratio except for 30 wt%. The composite with 30 wt% Cu could be completely exposed because the exposed thickness was the same as the spin-coated thickness of 30–40 μm. Although the evaluation of 10 and 20 wt% of composites were not performed, the exposed thickness could be near the spin-coated thickness in the same result as 30 wt% of composites. Therefore, it is

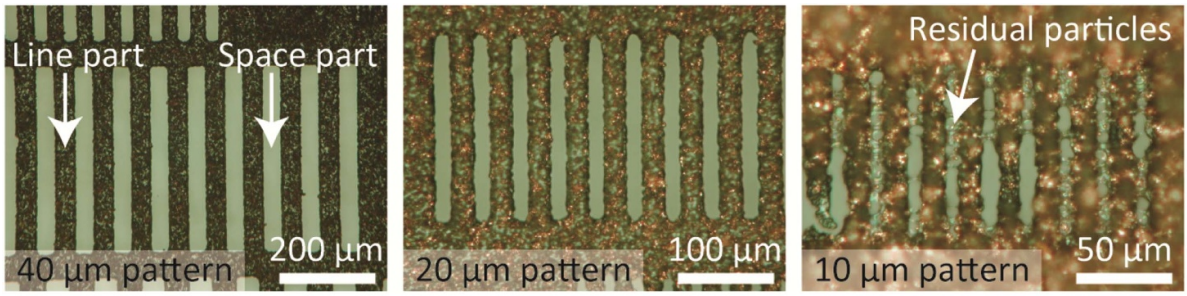

Figure 7. Observation images of line and space patterns fabricated with the composite (30 wt%) using 1 μm diameter Cu particles.

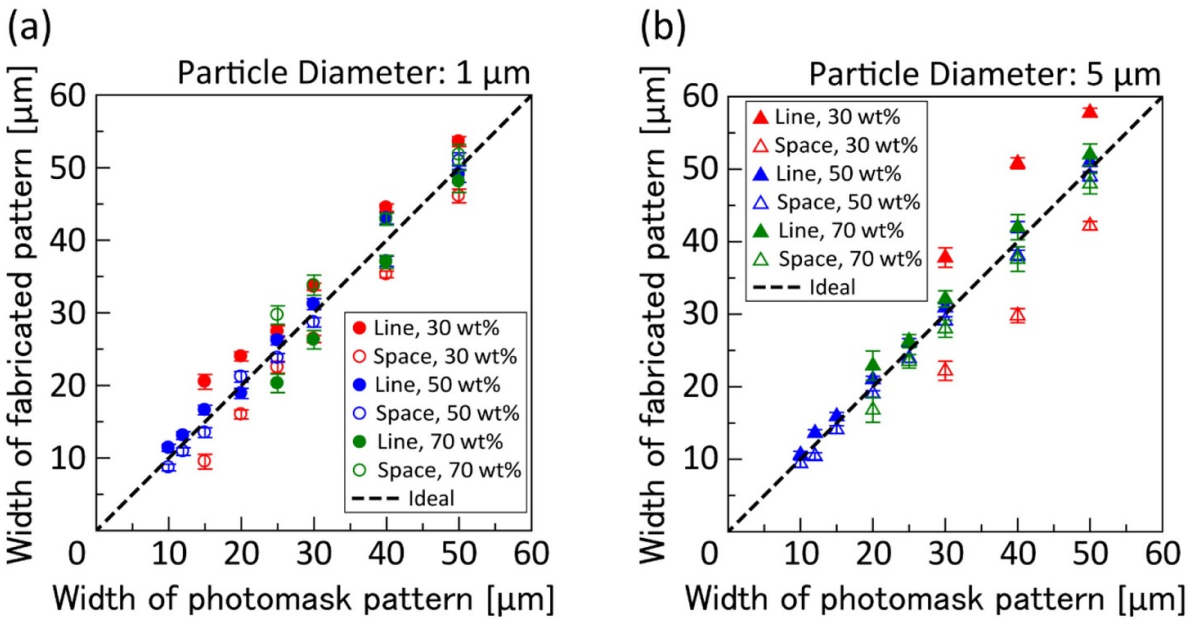

Figure 8. Measurement results of patterning accuracy for the composites. Patterning accuracy of the composites using (a) 1 μm diameter Cu particles; (b) 5 μm diameter Cu particles.

necessary to consider the limitation of exposed thickness when the composite of Cu 50 and 70 wt% was used for fabricating structures.

3.2. Evaluation of results for patterning accuracy of composites

Figure 7 shows the observation images of the fabricated line-and-space patterns using the composite with 30 wt% of 1 μm diameter Cu particles. Figure 8 shows comparison of the measurement results of the fabricated pattern width of the composites with the pattern width in the photomask, in which the x-axis is the pattern width in the photomask, and the y-axis is the measured width in the specimens. The width of the line patterns, except for the composite with 70 wt% and 1 μm particle size, were larger than those of the space patterns. As the exposure dose of the composites was larger than that of the conventional SU-8 process, the effects of diffracted light from the edge of the pattern in the photomask became dominant, which caused an increase in the width of the line patterns. The residual particles were observed in the space parts of the small patterns, as shown in figure 7. It is difficult to form

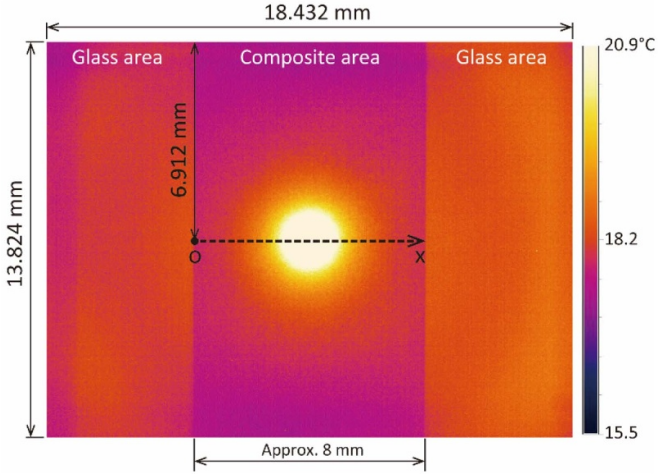

Figure 9. Observation image by the thermal camera set over the centre of the composite irradiated with green light.

small patterns using the composites because the width of the pattern becomes equal to the size of the Cu particles. In contrast, for the Cu 70 wt% composite with 1 μm diameter, the

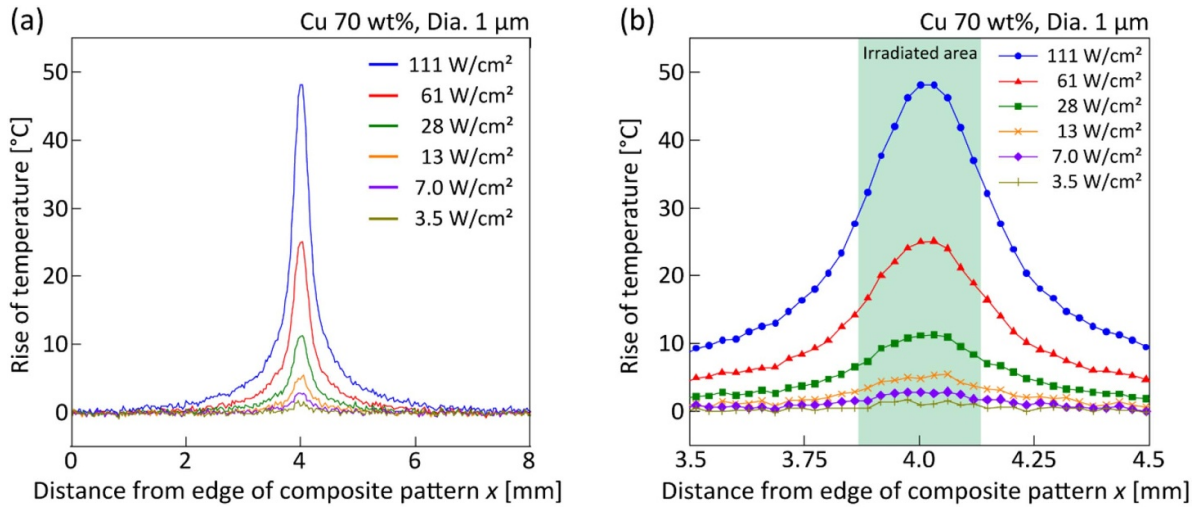

Figure 10. Evaluation results of photothermal effect of Cu 70 wt% composite with composite with 1 μm diameter particles. (a) X-axis is set from 0 to 8 mm, and the irradiated area is in the centre. (b) X-axis is set from 3.5 to 4.5 mm. The light green area is the light irradiated area.

line pattern was smaller than the space pattern, as shown in figure 8(a). In this condition, the mixed particles impeded the UV light, and the exposed parts of the line pattern decreased. The composites using 1 μm diameter Cu particles have patterning abilities of 15, 10, and 25 μm for weight ratios of 30, 50, and 70 wt%, respectively, as shown in figure 8(a). The patterning abilities of the composites using 5 μm in diameter Cu particles were 30, 10, and 20 μm for the weight ratio of 30, 50, and 70 wt%, respectively, as shown in figure 8(b). The other smaller width of patterns were not measured because the patterns were not formed. From these results, suitable doses according to the weight ratio of composites are required to produce microdevices, and the fabricated devices involve a dimensional error of 5%–25%. Although the patterning accuracy of 10 and 20 wt% composites were not evaluated in this study, the same dimensional error would be obtained by setting suitable doses for each conditions.

3.3. Evaluation results of photothermal effect

Figure 9 shows an example of an observation image by the thermography camera set above the centre of the composite irradiated with green light. In this figure, the specimen of Cu 70 wt% was used and the irradiance was 111 W cm^{-2}. To explain the rise of temperature, the displayed temperature range of thermography camera was set between 15.5 °C and 20.9 °C. There was a difference in temperature of approximately ±2 °C between glass and composite regions. Although the thermography camera was calibrated for a black body with 1.0 in emissivity, a measurement error could be included in this experiments due to the difference of the emissivities between the glass and composite. The obtained temperature data was used to calculate a rise of temperature, which indicates the difference between the temperature at no irradiation and the temperature obtained at light irradiation. Figure 10(a) shows the rise of temperature obtained using the composite with Cu 70 wt% of 1 μm diameter particles. In this graph, the x-axis is the distance from the edge of the composite pattern, and the y-axis is the rise of temperature. Figure 10(b) shows the measurement results enlarged at the range of the x-axis from 3.5–4.5 mm, as shown in figure 10(a). Measurement results of other composites were shown in supporting information (figures S1–S9 (available online at stacks.iop.org/JMM/31/095007/mmedia)). The maximum rise of temperature was observed at the centre of the irradiated area and increased with the increase in irradiance. Figure 11 shows the measured temperatures (mean ± standard deviation, $N = 5$) of composite with Cu 70 wt% for the change in irradiance at the centre of irradiated area. The rise of temperature almost linearly increased with the increase in irradiance. This property is caused by the Cu particles in composites, which could be excited linearly for the irradiance [24]. Therefore, the control of temperature on the composites was performed by controlling the irradiance. Figure 12 shows the rise of temperature (mean ± standard deviation, $N = 5$) at 111 W cm^{-2} in irradiance for the change in the weight ratio of Cu particles. The temperature of the composite increased with increasing weight ratio up to 50 wt% and decreased at a weight ratio of 70 wt%. The rise of the temperature of the 70 wt% composite using 1 μm diameter Cu particles was smaller than that of the 50 wt% composite because the thickness of the 70 wt% composite was smaller than that of the other composites. The measurement results of thickness were available in the supporting information (table S1). Because the thickness affects the thermal capacity of the composite, composites with thin thicknesses were unable to retain the induced heat by light irradiation. In addition, the temperature of composites might be decreased by the increase of thermal conductivity of the composites with increase of the weight ratio of Cu particles. In our experiments, the maximum temperature (55.7 °C) was obtained at the 50 wt% composite using 1 μm diameter Cu particles. In contrast, there is no change in rise of temperature (0.6 °C) on the SU-8 pattern without Cu particles at irradiance of 111 W cm^{-2}.

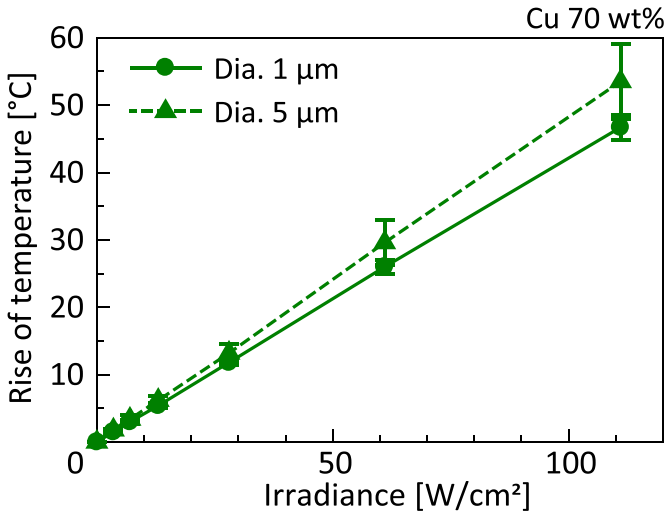

Figure 11. Measurement results of rise of temperature for the change in irradiance.

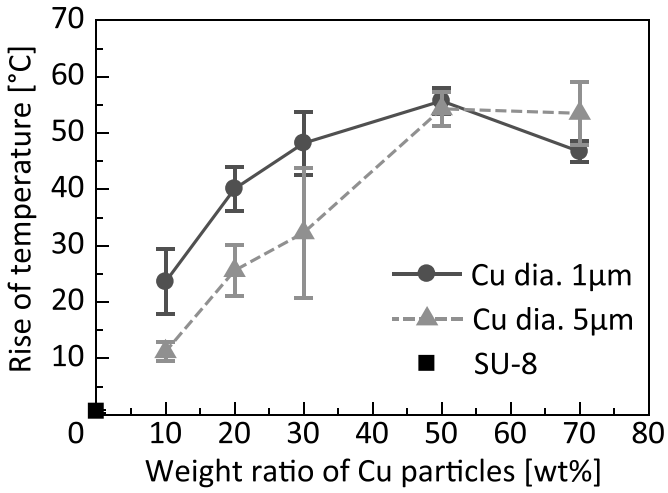

Figure 12. Rise of temperature for the change in weight ratio of Cu particles.

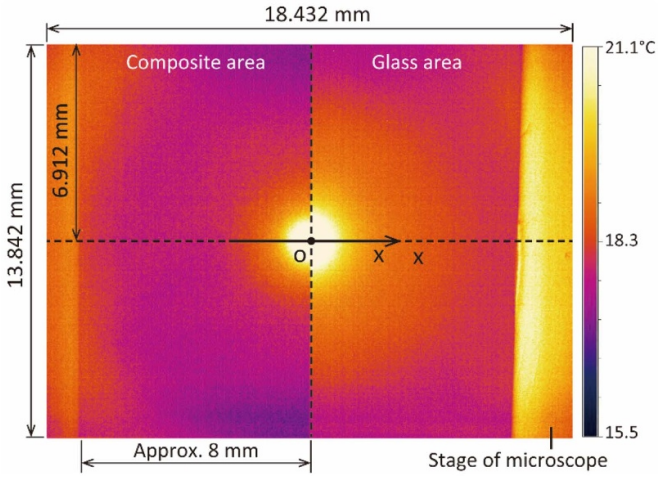

Figure 13. Observation image of the thermal camera set over the boundary between the composite pattern and glass area.

Figure 13 shows an example of an observation image by the thermography camera set over the boundary between the composite structure and the glass area. The excitation light was irradiated at the boundary. Figures 14(a) and (b) show the results of the rise of temperature for the composites using 1 and 5 μm diameter Cu particles, respectively. In these graphs, the boundary is set as the origin, and the x-axis is set as the distance from the boundary. The rises of temperature of the composites including Cu of 30, 50, and 70 wt% were almost the same at the boundary. Since thermal conductivity is in proportion to the difference of temperature, the temperature of Cu 70, 50 wt% composite, which showed a higher rise of temperature, might be decreased significantly its temperature in the boundary between composite and glass area. The heat generated in the composite was applied to the glass area. In the glass area at a distance of 28.8 μm, which is the closest distance from the boundary in this experiments, rises of temperature of 15.1 °C and 15.2 °C were obtained for the composite with 70 wt% Cu particles of which sizes are 1 and 5 μm, respectively. The composites with Cu of 30 and 50 wt% also showed a rise of temperature over 10 °C in the same area. Therefore, structures made of this composite could be used in applications that require a rise of temperature to ∼10 °C for such as the control activity of proteins or the control of thermoresponsive polymers [25–27].

3.4. *Evaluation results of microheater*

Figures 15(a) and (b) show the observation images before and after irradiation for the fabricated composite structure of circular pattern with a diameter of 100 μm. The designed composite structures were formed, and a rise of temperature was observed (available in the supporting information movie). Since the fluctuation of the temperature was small during the excitation, the microheater has a stability of temperature. The thickness of the structures was approximately 7 μm. Figure 16 shows the measurement results of the rise of temperature (mean ± standard deviation, $N = 3$) for each diameter of the circular structures. The structures with diameters of 100 μm and 200 μm showed a rise of temperature of 16.1 °C and 38.6 °C, respectively. The rise of temperature was constant at approximately 46 °C in structures with a diameter over 400 μm. The difference in the temperature between the structure sizes may be attributed to the area of light absorption. As the structures with a diameter lower than 200 μm were smaller than the irradiated area of approximately 265 μm in diameter, the rise of temperature became lower than those of the other sizes of structures. Figure 17 shows the measured temperature at switching irradiance between 0 and 111 W cm^{-2}. The temperature on the composite changed according to the switch of irradiance, and reached an almost constant temperature after

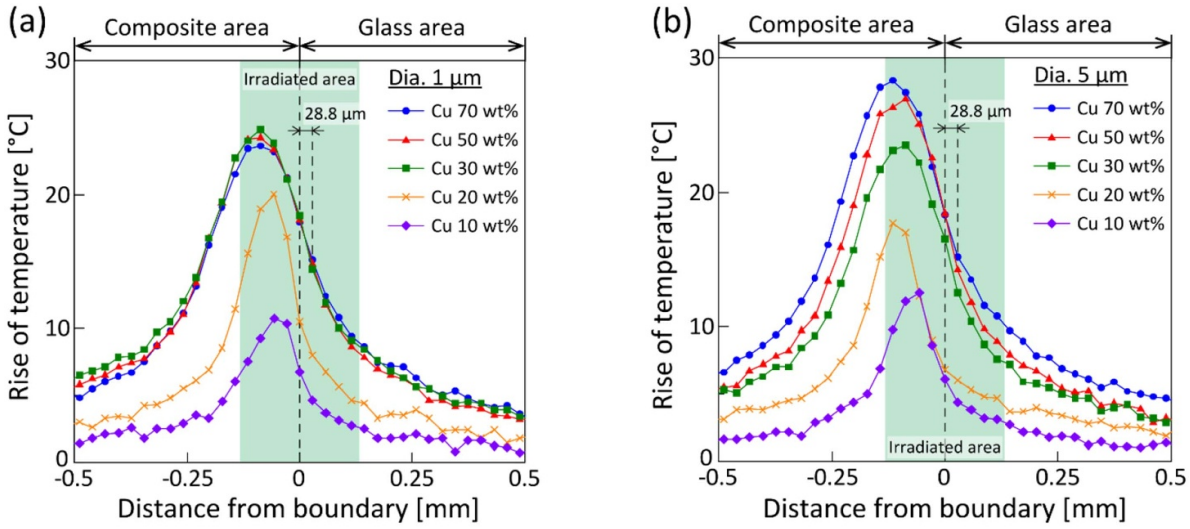

Figure 14. Evaluation results of photothermal effect at the boundary between the composite and the glass area. Measurement results of composites using (a) 1 μm diameter Cu particles; (b) 5 μm diameter Cu particles.

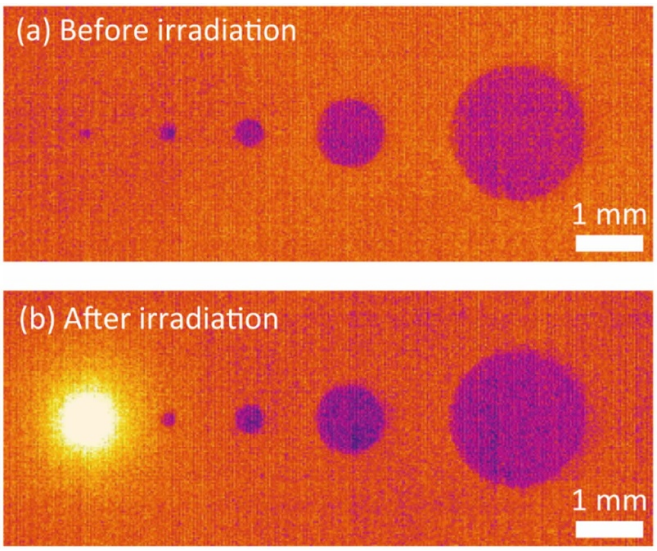

Figure 15. Observation images (a) before and (b) after irradiation for the fabricated circular structure.

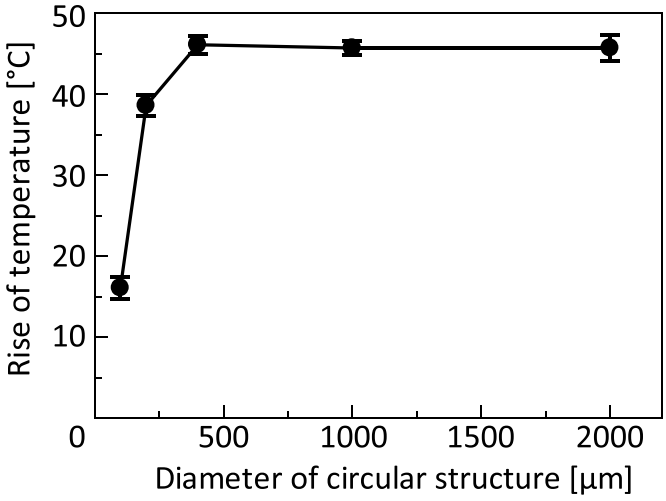

Figure 16. Measurement result of rise of temperature for the change in the diameter of circular structure.

1 s from the start of irradiation. The time response of proposed microheater is equivalent to the photothermally actuated heater reported in previous study [2, 9]. The efficiency of microheater from light energy to thermal energy was calculated to be 32% (see the supporting information) [23, 24, 28, 29]. From these results, the fabricated composite structure demonstrated the characteristics of a microheater, which has stability for the excitation light. In case of irradiating excitation light, which is larger than a size of micropattern, the rise of temperature can be selectively obtained near the micropattern. However, an improvement method for such as an increasing in the thickness of the composite is required to increase the rise of temperature. The experiments for a life-time and durability of microheater are required to demonstrate its reliability. Although the maximum temperature and the response time of proposed microheater is smaller than a previously reported electrical resistance heater [30, 31], its heating area can be controlled flexibly by setting the irradiated area of excitation light. Moreover, proposed microheater is fabricated by one step photolithography, which means simpler fabrication process. The proposed microheater could be applicable for such as control activity of proteins, control of thermoresponsive polymer, and driving thermo-pneumatic micropump [25–27, 32]. In addition, patterned microstructure could be useful for physically control of the moving direction in the motility assay of proteins [33].

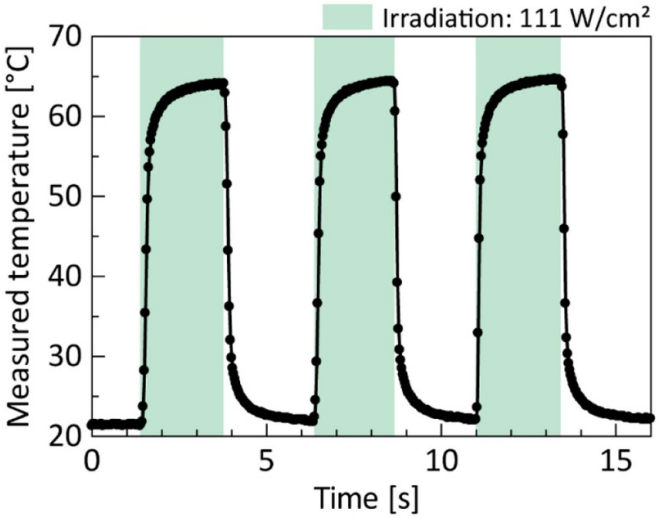

Figure 17. Measured temperature at switching irradiance between 0 and 111 W cm^{-2}.

4. Conclusions

In this study, we proposed a microheater using the photothermal effect of the SU-8/Cu composite. To evaluate the patterning characteristics of the composites by photolithography, we measured the transmittance and the exposed thickness. The measured transmittances and the exposed thicknesses decreased with an increase in the weight ratio of the Cu particles of the composites. In the evaluation of patterning accuracy of the composites, although the minimum size of line-and-space pattern formed was 30 μm, the fabricated patterns involved a dimensional error of 5%–25%. In the evaluation of the photothermal effect of composites, the temperature rise was controlled by the green-light irradiance. The composite with 50 wt% of 1 μm Cu particles showed the maximum rise of temperature of 55.7 °C in our experiments. Then, the rise of temperature over 10 °C was measured at the glass area at a distance of 28.8 μm from the edge of the composite structure (30, 50, 70 wt% Cu). The fabricated microheaters with the diameters from 100 to 2000 μm showed a rise of temperature. The temperatures increased by 16.1 °C and 38.6 °C for the microheater with diameters of 100 and 200 μm, respectively. The other microheaters showed a constant value of approximately 46 °C. In addition, the response time of rising temperature was approximately 1 s. From these results, the proposed microheater could be useful for applications that require a rise of temperature within 10 °C–40 °C for such as the control activity of proteins, the control of thermoresponsive polymers, or the lab-on-a-chip applications.

Data availability statement

All data that support the findings of this study are included within the article (and any supplementary files).

Acknowledgments

This work was partially supported by JSPS KAKENHI, Grant No. JP20H02117, and MEXT 'Nanotechnology Platform Program', Grant Number JPMXP09F20YA0009. We would like to thank Editage (www.editage.com) for English language editing.

ORCID iD

Tasuku Nakahara https://orcid.org/0000-0001-8969-2776

References

[1] Wang T, Torres D, Fernández F E, Wang C and Sepúlveda N 2017 Maximizing the performance of photothermal actuators by combining smart materials with supplementary advantages *Sci. Adv.* **3** e1602697–e
[2] Zhang X *et al* 2014 Photoactuators and motors based on carbon nanotubes with selective chirality distributions *Nat. Commun.* **5** 2983
[3] Kim B, Han M and Kim E 2019 Photothermally powered conductive films for absorber-free solar thermoelectric harvesting *J. Mater. Chem.* A **7** 2066–74
[4] Nakahara T, Ikuta J, Shintaku H, Kotera H and Yokokawa R 2014 *In situ* velocity control of gliding microtubules with temperature monitoring by fluorescence excitation on a patterned gold thin film *Mater. Res. Express* **1** 045405
[5] Hiremath S, H S M, H S M and Kulkarni S M 2021 Progression and characterization of polydimethylsiloxane-carbon black nanocomposites for photothermal actuator applications *Sens. Actuators* A **319** 112522
[6] Wang X, Dai L, Jiao N, Tung S and Liu L 2021 Superhydrophobic photothermal graphene composites and their functional applications in microrobots swimming at the air/water interface *Chem. Eng. J.* **422** 129394
[7] Wang E, Desai M S and Lee S-W 2013 Light-controlled graphene-elastin composite hydrogel actuators *Nano Lett.* **13** 2826–30
[8] Zhu Z, Senses E, Akcora P and Sukhishvili S A 2012 Programmable light-controlled shape changes in layered polymer nanocomposites *ACS Nano* **6** 3152–62
[9] Zhang X *et al* 2011 Optically- and thermally-responsive programmable materials based on carbon nanotube-hydrogel polymer composites *Nano Lett.* **11** 3239–44
[10] Hauser A W, Evans A A, Na J-H and Hayward R C 2015 Photothermally reprogrammable buckling of nanocomposite gel sheets *Angew. Chem., Int. Ed.* **54** 5434–7
[11] Liu J, Cai B, Zhu J, Ding G, Zhao X, Yang C and Chen D 2004 Process research of high aspect ratio microstructure using SU-8 resist *Microsyst. Technol.* **10** 265–8
[12] Lin C-H, Lee G-B, Chang B-W and Chang G-L 2002 A new fabrication process for ultra-thick microfluidic microstructures utilizing SU-8 photoresist *J. Micromech. Microeng.* **12** 590–7
[13] Jiguet S, Bertsch A, Hofmann H and Renaud P 2004 SU8-silver photosensitive nanocomposite *Adv. Eng. Mater.* **6** 719–24
[14] Damean N, Parviz B A, Lee J N, Odom T and Whitesides G M 2005 Composite ferromagnetic photoresist for the fabrication of microelectromechanical systems *J. Micromech. Microeng.* **15** 29–34

[15] Peters C, Ergeneman O, Sotiriou G A, Choi H, Nelson B J and Hierold C 2015 Visible light curing of Epon SU-8 based superparamagnetic polymer composites with random and ordered particle configurations *ACS Appl. Mater. Interfaces* **7** 193–200
[16] Voigt A, Heinrich M, Martin C, Llobera A, Gruetzner G and Perez-Murano F 2007 Improved properties of epoxy nanocomposites for specific applications in the field of MEMS/NEMS *Microelectron. Eng.* **84** 1075–9
[17] Suzuki J, Onishi Y, Terao K, Takao H, Shimokawa F, Oohira F, Miyagawa H, Namazu T and Suzuki T 2016 Development of a two-dimensional scanning micro-mirror utilizing magnetic polymer composite *Japan. J. Appl. Phys.* **55** 6
[18] Suter M, Ergeneman O, Zürcher J, Moitzi C, Pané S, Rudin T, Pratsinis S E, Nelson B J and Hierold C 2011 A photopatternable superparamagnetic nanocomposite: material characterization and fabrication of microstructures *Sens. Actuators* B **156** 433–43
[19] Kandpal M, Sharan C, Palaparthy V, Tiwary N, Poddar P and Rao V R 2015 Spin-coatable, photopatternable magnetic nanocomposite thin films for MEMS device applications *RSC Adv.* **5** 85741–7
[20] Suter M, Zhang L, Siringil E C, Peters C, Luehmann T, Ergeneman O, Peyer K E, Nelson B J and Hierold C 2013 Superparamagnetic microrobots: fabrication by two-photon polymerization and biocompatibility *Biomed. Microdevices* **15** 997–1003
[21] Nakahara T, Suzuki J, Hosokawa Y, Shimokawa F, Kotera H and Suzuki T 2018 Fabrication of magnetically driven microvalve arrays using a photosensitive composite *Magnetochemistry* **4** 7
[22] Nakahara T, Ueda Y, Miyagawa H, Kotera H and Suzuki T 2020 Self-aligned fabrication process for active membrane in magnetically driven micropump using photosensitive composite *J. Micromech. Microeng.* **30** 25006
[23] Chen S, Tang F, Tang L and Li L 2017 Synthesis of Cu-nanoparticle hydrogel with self-healing and photothermal properties *ACS Appl. Mater. Interfaces* **9** 20895–903
[24] Roper D K, Ahn W and Hoepfner M 2007 Microscale heat transfer transduced by surface plasmon resonant gold nanoparticles *J. Phys. Chem.* C **111** 3636–41
[25] Böhm K J, Stracke R, Baum M, Zieren M and Unger E 2000 Effect of temperature on kinesin-driven microtubule gliding and kinesin ATPase activity *FEBS Lett.* **466** 59–62
[26] Korten T, Birnbaum W, Kuckling D and Diez S 2012 Selective control of gliding microtubule populations *Nano Lett.* **12** 348–53
[27] Tsuda Y, Kikuchi A, Yamato M, Chen G and Okano T 2006 Heterotypic cell interactions on a dually patterned surface *Biochem. Biophys. Res. Commun.* **348** 937–44
[28] Ding X *et al* 2014 Surface plasmon resonance enhanced light absorption and photothermal therapy in the second near-infrared window *J. Am. Chem. Soc.* **136** 15684–93
[29] Lai J-L, Liao C-J and Su G-D 2012 Using an SU-8 photoresist structure and cytochrome C thin film sensing material for a microbolometer *Sensors* **12** 16390–403
[30] Nguyen D M, Hu L, Miao J and Ohl C-D 2018 Oscillate boiling from electrical microheaters *Phys. Rev. Appl.* **10** 044064
[31] Xu T, Miao J, Li H and Wang Z 2009 Local synthesis of aligned carbon nanotube bundle arrays by using integrated micro-heaters for interconnect applications *Nanotechnology* **20** 295303
[32] Chee P S, Minjal M N, Leow P L and Ali M S M 2015 Wireless powered thermo-pneumatic micropump using frequency-controlled heater *Sens. Actuators* A **233** 1–8
[33] Hiratsuka Y, Tada T, Oiwa K, Kanayama T and Uyeda T Q P 2001 Controlling the direction of kinesin-driven microtubule movements along microlithographic tracks *Biophys. J.* **81** 1555–61